

# Leakage Detection in Buried Pipes by Electrical Resistance Imaging

Josep Jordana, Manel Gasulla and Ramón Pallás-Areny

Divisió d'Instrumentació i Bioenginyeria, Departament d'Enginyeria Electrònica  
Universitat Politècnica de Catalunya  
Jordi Girona 1-3, Edifici C-4  
08034 Barcelona, SPAIN  
Phone 34-93-401-7483 Fax 34-93-401-6756  
E-mail: jordana@eel.upc.es

**Abstract:** *This work describes a non-invasive method to detect leaks in buried pipes that uses a surface linear electrode array perpendicular to the pipe axis. Two electrodes inject current and the remaining electrodes detect the drop in voltage. We have used both the dipole-dipole array and a modified Schlumberger array.*

*A single step reconstruction algorithm based on the sensitivity theorem yields 2D images of the cross section. The corresponding sensitivity matrices are ill-posed. Nevertheless, the reconstructed images allow us to detect leaks without needing any regularisation parameter because it is possible to replace the inverse of the sensitivity matrix by their transposed.*

*A personal computer controls current injection, electrode switching and voltage detection, which enables us to easily test different electrode arrays. The system has been first tested in the laboratory using a stainless steel tube immersed in water and covered by a rubber sleeve to simulate a non-conductive leak. By taking reference measurements with the immersed bare pipe, it is possible to reconstruct images showing the simulated leak using 16 electrodes and even 8 electrodes only, though with reduced resolution.*

*Field measurements have involved simulated water leaks from a 1 m plastic tube, 8 cm in radius buried at about 24 cm depth in a farm field. The system injected 1 kHz, 20 V peak-to-peak square waveforms, thus avoiding electrode polarisation effects. Images reconstructed from an eight-electrode array show the leak if the image before the leak is used as reference.*

**Keywords:** Geoelectrics, resistance tomography, leak detection, synchronous sampling.

## 1. INTRODUCTION

Electrical resistivity surveying is a versatile prospecting method applicable to groundwater location, archaeological evaluation and contaminant monitoring. It is a common method in shallow subsurface investigations, especially for groundwater studies [1]. Leak detection methods based on soil sampling and borehole tomography are expensive. Hence, we are considering subsurface resistivity measurements to detect leakage from buried pipes because they do not need soil drilling.

Tomographic imaging of geophysical data has become increasingly important because of the need for a high-resolution approach to delineate buried structures, mainly in near-surface exploration. Resistance tomography is gaining importance as alternative to soil studies based on apparent resistivity curves. This advance is fueled by progress in instrumentation and data processing.

Electrical impedance tomography (EIT) aims to image impedance distribution in an object's cross section from surface measurements. EIT arose in medical imaging but has found broader application in industrial processes. Dines and Lytle [2] proposed EIT for geophysical applications.

Measurements in inverse geophysical problems are not very sensitive to target parameters. As a result, inverse geophysical problems are unstable, and two different targets can yield similar measurements. Therefore, the aim is to find an approximate solution, as close as possible to the actual situation. Regularisation tools help in those inversion problems. According to Tikhonov and Goncharsky [3], the efficiency in geophysical prospecting depends more on the efficiency in data processing and interpretation than on more accurate instrumentation. Resistive geoelectrical prospecting often uses stratified models because many geophysical cross sections consist of homogeneous layers with given resistivity and thickness [4].

In any tomography system, an image reconstruction algorithm obtains images from the measured data. There are several 2D algorithms able to image underground resistivity distributions. Many of them derive from EIT for medical applications [5] [6]. Noel and Xu [7] proposed an algorithm to image shallow underground objects, applicable to archaeology.

Using matrices, an inverse problem can be described by

$$G m = d \quad (1)$$

where  $d = [d_1, d_2, \dots, d_M]^t$  is the data vector,  $m = [m_1, m_2, \dots, m_P]^t$  is the parameter vector (target), and  $G$  is the Jacobian matrix [8] or data Kernel, whose order is  $M \times P$ .

Geophysical data inversion aims to estimate the parameters of an earth model from a series of observations. Often, there is not a single solution and two or more solutions fit the observations within a given error margin.

Geophysical models consider several ground layers or strata, whose thickness and resistivity must be determined. There are several inversion techniques tailored to those models, which are based on fitting measured to theoretical apparent resistivity profiles [4]. Noel and Xu [7] image two-layer distributions using a reconstruction algorithm based on electrical resistivity tomography (ERT).

Solving (1) by the least-squares method yields an estimate

$$m^{est} = (G^t G)^{-1} G^t d \quad (2)$$

This solution, termed Gauss-Newton solution [8], suits equation systems that are overdetermined, i.e., there are more observations than parameters in the model ( $M > P$ ). In order to achieve an acceptable solution using the least-squares method, underdetermined systems need additional (a priori) information [9]. This inversion problem is in trouble when  $G^t G$  is a singular matrix.

$G$  is an ill-conditioned matrix and this compounds the problem because small data variations affect image reconstruction. Hence, measurement noise modifies model parameters according to

$$G(m + \Delta m) = d + \Delta d \quad (3)$$

The relative sensitivities of measured data and parameter models are related by the *condition number* of  $G$ ,  $\text{cond}(G)$ , [10] according to

$$\frac{|\Delta m|}{|m|} \leq \text{cond}(G) \frac{|\Delta d|}{|d|} \quad (4)$$

where  $\text{cond}(G) = \mu_1 / \mu_N$ , and  $\mu_1$ ,  $\mu_N$  are, respectively the largest and the smallest eigenvalues of  $G$ . From (4), the largest  $\text{cond}(G)$  is, the worst the influence of measurement noise on calculated model parameters. Lascaux and Theodor [11] analyse matrix conditioning and solve different problems using the least-squares method.

In order to alleviate some of the difficulties in inverting  $G^t G$ , we solve an alternative problem using the least-squares method. Many inverse problems are neither completely determined nor completely underdetermined. Their solution can be then written as [9]

$$m^{est} = (G^t G + I \lambda)^{-1} G^t d \quad (5)$$

The damping factor  $\lambda$  attenuates the contribution of the underdetermined part to the solution. This method, termed Marquardt-Levenberg [8] overcomes the difficulty in inverting  $G^t G$  because  $\lambda$  prevents singularities by offsetting values in the diagonal of  $G^t G$ , so that any of them is zero.

Loke and Torleif [12] compare different iterative methods to invert geoelectric data using the least-squares method. The Marquardt-Levenberg algorithm yields a distorted solution when there are many parameters. Furthermore, the solution depends on  $\lambda$ . We are interested on reconstruction algorithms that do not need any regularisation parameter and that are not iterative, thus saving computation time.

## 2. IMAGING ALGORITHM

Imaging subsurface resistivity distributions needs the placement of a series of electrodes for current injection and voltage detection. Figure 1 shows electrode placement to image successive vertical image distributions. Electrodes A and B constitute injection pair  $m$  and electrodes M and N are detection pair  $n$ .

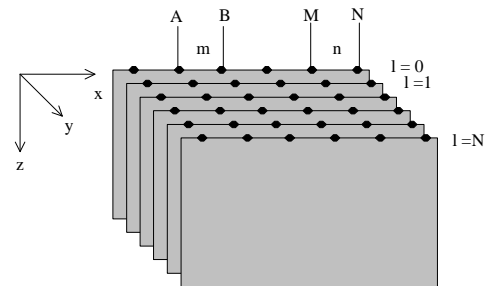


Figure 1: Electrode arrangement for imaging vertical, underground resistivity distributions.

In order to solve the inverse problem in (1), we need to know G, which characterises the medium. G is termed sensitivity matrix because its coefficients result from applying the sensitivity theorem [13].

The proposed algorithm relies on the following assumptions:

- Measured data is the real part of the impedance. Hence, images correspond to underground conductivity or resistivity distributions.

- Electrode separation is uniform.

- The initial conductivity distribution is assumed to be uniform.

- Conductivity changes to be imaged are not very different from the uniform distribution. Nevertheless, the algorithm can detect high-contrast anomalies.

- The region to image is bidimensional.

Practical situations do not met all the above assumptions. In medical applications, for example, the electrical conductivity in a cross section of the human body is not uniform. Nevertheless, several authors have obtained useful images [5] [6]. We propose to use the algorithm developed by Kotre [6] because it is fast and does not need any regularisation parameter.

According to [6] when the resistivity changes, the change in voltage corresponding to an injecting-detecting electrode pair  $m-n$  as a function of the sensitivity coefficients obeys to

$$\left( \frac{V - V_h}{V_h} \right)_{m,n} = \frac{\sum_x \sum_y \sum_z S_{m,n,x,y,z} \left( \frac{r - r_h}{r_h} \right)_{(x,y,z)}}{\sum_x \sum_y \sum_z S_{m,n,x,y,z}} \quad (6)$$

$V$  are the measured voltages when there is the anomaly,  $V_h$  are the measured voltages for an homogeneous medium and  $S_{m,n,x,y,z}$  is the sensitivity coefficient relating the measurement (m,n) to the position (x,y,z). For several injecting-detecting pairs, (6) leads to an equation system relating small conductivity changes to voltage changes measured on the surface.

The normalised resistivity is then [14]

$$P(x, y, z) = \frac{\sum_m \sum_n S_{m,n,x,y,z} \left( \frac{V - V_h}{V_h} \right)_{(m,n)}}{\sum_m \sum_n S_{m,n,x,y,z}} \quad (7)$$

This reconstruction method approximates the inverse sensitivity matrix by its transposed, whose values (reconstructed pixels) are

$$P(x, y, z) = \ln(r(x, y, z)) - \ln(r_h) \quad (8)$$

where  $r_h$  is the reference resistivity (homogeneous medium) and  $r(x, y, z)$  is the actual resistivity distribution, slightly different from the homogeneous distribution. Some experimental measurements later described involve high-contrast objects, but the algorithm detects them too.

The initial algorithm was intended for medical applications involving a circular perimeter [14]. Later, Kotre [15] considered geoelectric applications and the detection of abandoned land mines [16].

This reconstruction algorithm yields blurred images that can be restored by a spatial frequency filter derived from the algorithm's *point-spread-function* (PSF). Image restoration is particularly useful to image strata parallel to the measurement surface [15]. Leak detection, however, only needs to distinguish between images showing an intact pipe and images showing a leaking pipe. There is no need for neat images, and experimental results without any restoration filter are acceptable.

### 3. INSTRUMENTATION

Figure 2 shows the instrumentation system that we have designed for field measurements. A function generator (HP3245A) injects a 1 kHz, 20 V peak-to-peak square waveform. Synchronously sampling the flat zone of square signals reduces interference [17]. The voltage detector [18] implements synchronous demodulation using the floating capacitor technique [19]. A portable PC controls this detector via the serial port (EIA232). A Daqbook-120 plug-in card (Iotech) acquires the demodulated dc voltage. The portable computer also controls four switching plug-in cards with 8 relays each that allow us to implement any injection-detection strategy using 8 electrodes [20].

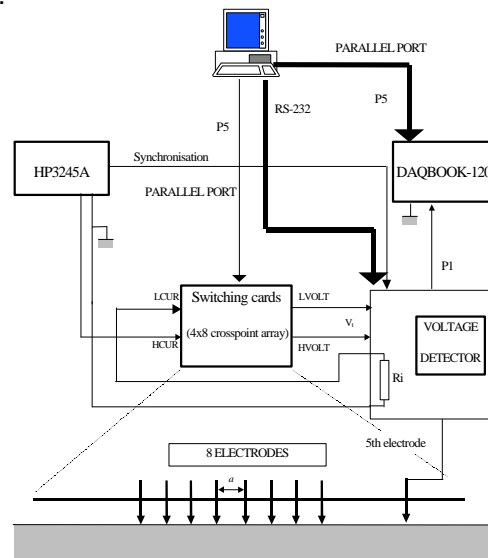


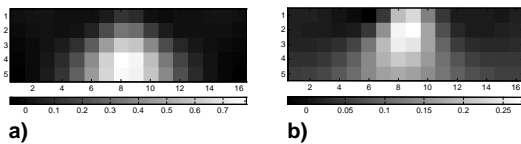
Figure 2: Measurement system for current injection and voltage detection.

### 4. EXPERIMENTAL MEASUREMENTS

The reconstruction algorithm has been first tested in the laboratory by immersing different objects into a 40 cm x 30 cm x 25 cm water tank. A non-conductive sleeve (rubber) around a cylindrical conductor simulates a leaking pipe [21]. The cylinder radius was 2 cm and the immersion depth 4 cm. Gasulla et al. [22] describe the measurement system used in the laboratory.

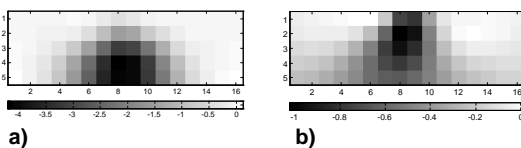
We have considered two different electrode arrays: dipole-dipole, including end electrodes, and a modified Schlumberger array [23], using 16 and 8 electrodes uniformly spaced along the same distance (30 cm).

Figure 3 shows the reconstructed cylinder using 16 electrodes. Both electrode arrays yield similar images, in spite of the larger number of independent measurements for the dipole-dipole array (104) than for the modified Schlumberger array (91).



**Figure 3:** Reconstructed image for a metal cylinder 2 cm in radius immersed 4 cm in water, from voltages measured with 16 electrodes spaced 2 cm, using a) the dipole-dipole array and b) the modified Schlumberger array.

Figure 4 shows the corresponding images when a rubber sleeve 0.5 thick covers the cylinder in figure 3.

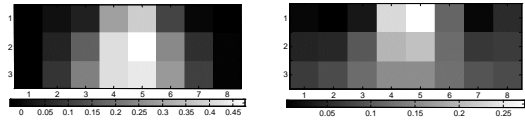


**Figure 4:** The reconstructed images for the cylinder in figure 3 change when a 0.5 cm rubber sleeve covers the cylinder.

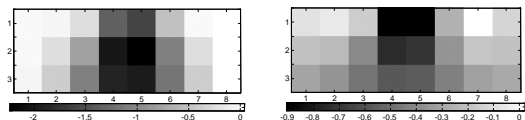
Figures 3 and 4 show that both electrode arrays allow us to detect a simulated leak, even though the modified Schlumberger array places the anomaly (cylinder) closer to the surface and the dipole-dipole array places the anomaly deeper. Reference voltages in figure 4 are those leading to figure 3, i.e., correspond to a medium that includes the pipe. This resembles the actual situation because it is impossible to obtain reference voltages corresponding to a medium without pipe (“homogeneous” medium). It would certainly be possible to take a reference

measurement far from the pipe. Nevertheless, the uncertainty in electrode placement yields large errors. Sánchez [24] has shown that images obtained from voltage changes relative to a homogeneous medium yield similar images.

Using 8 electrodes instead of 16 electrodes yields lower-resolution images. Nevertheless, figures 5 and 6 respectively show that it is possible to detect the pipe and the leak.



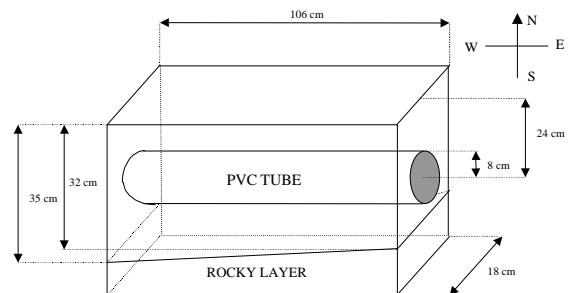
**Figure 5:** Reconstructed images for a metal cylinder 2 cm in radius immersed 4 cm in water, from voltages measured with 8 electrodes spaced 4 cm, using a) the dipole-dipole array and b) the modified Schlumberger array.



**Figure 6:** The reconstructed images for the cylinder in figure 5 change when a 0.5 cm rubber sleeve covers the cylinder.

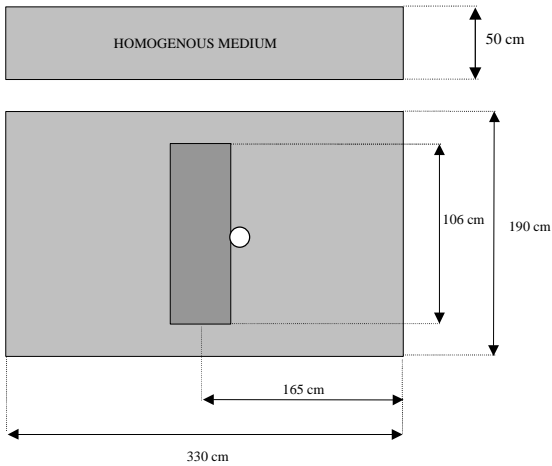
Images worsen for deeper objects. The algorithm allows us to detect leaks from pipes buried at four times the inter-electrode distance approximately [24].

We have carried out field measurements at a farm in Sta Eulàlia de Ronçana (Barcelona, Spain). We buried a PVC tube 106 cm in length and 8 cm in radius, at a 24 cm depth (figure 7). The top soil was about 35 cm thick and rested on rocky layer slightly tilted towards the west.



**Figure 7:** Tube dimensions and arrangement for field measurements.

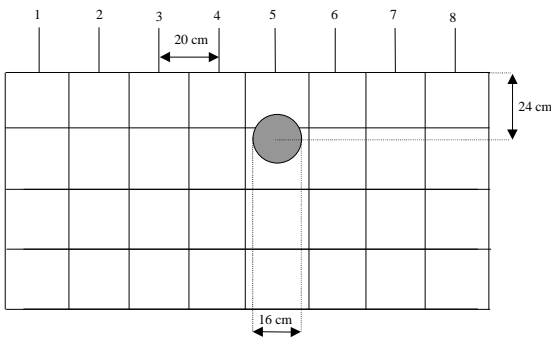
Because the soil was extremely dry, we watered a 1.9 m x 3.3 m area around the tube using about 32 l/m<sup>2</sup> (figure 8). A close area measuring 3.3 m x 0.5 m provided reference measurements. This reference area does not include any know object.



**Figure 8: Top view of the tube placement in the experimental field. The circle next to the tube shows the site of the simulated leak.**

The measurement system was that in figure 2 using 8 stainless-steel electrodes 20 cm in length and 1 cm in diameter inserted about 5 cm in the ground and spaced 20 cm.

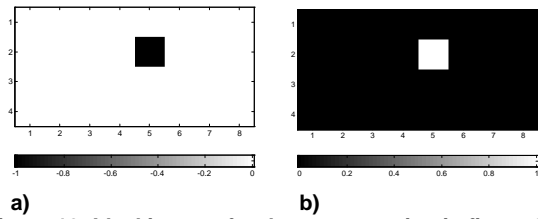
Figure 9 shows a vertical section across the tube and its position relative to the electrode array. The section is divided in 32 square pixels 20 cm in side. The tube is under the fifth electrode and belongs to two pixels. However, given that most of the tube falls inside the second row of pixels, the reference (ideal) image is that in figure 10, which shows both an insulating anomaly (PVC tube) and a conductive anomaly (water).



**Figure 9: Tube position, electrode array and pixel assignment for the vertical cross section to image.**

Pouring 10 l of water into a tube 7 cm in diameter that reached the buried tube from the surface (figure 8) simulated the leak. Because of terrain tilt, most of the water accumulated at the west of the buried tube.

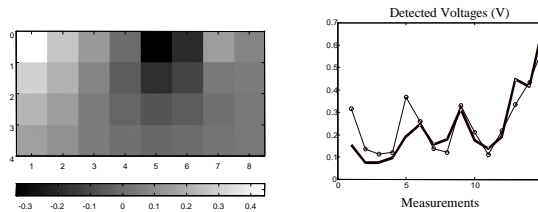
We used two electrode arrays: a modified Schlumberger array (15 independent voltage measurements) and dipole-dipole with end-electrode measurements (20 independent voltage measurements).



**Figure 10: Ideal images for the cross section in figure 9. a) Insulating object. b) Conductive object.**

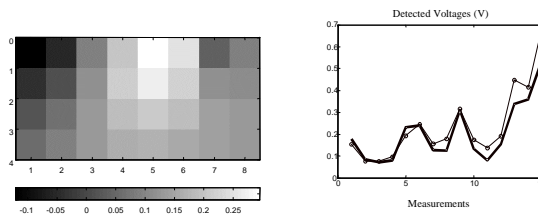
#### 4.1 Results with the modified Schlumberger array

Figure 11 shows the detected voltages using the modified Schlumberger array and the reconstructed image for the buried tube. The circles, joined by a thin line, correspond to the voltages detected in the reference area. The thick line corresponds to the voltages measured along an imaginary surface line across the tube centre and perpendicular to its axis.



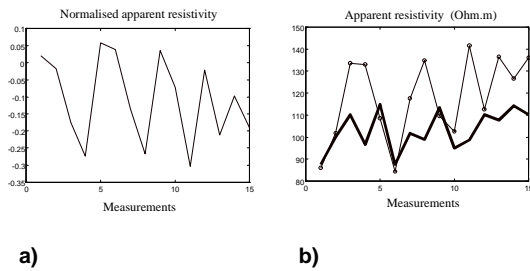
**Figure 11: a) Reconstructed image for the buried tube using the modified Schlumberger array. b) Measured voltages in the homogeneous area (circles) and along a surface line across the tube.**

Figure 12 shows the image corresponding to the simulated water leak. The change in colour with respect to figure 11 for the pixels close to the area where there is the tube, suggest a medium more conductive than the insulating tube.

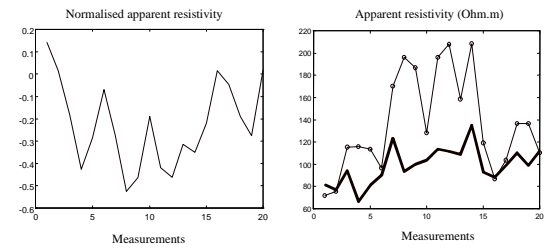


**Figure 12: a) Reconstructed image for the leak using the modified Schlumberger array. b) Measured voltages when there is a conductive leak (thick line).**

Figure 13 shows apparent resistivities for the tube alone and for the tube plus the simulated leak, and the normalised apparent resistivity. Negative values imply that the leak is conductive.



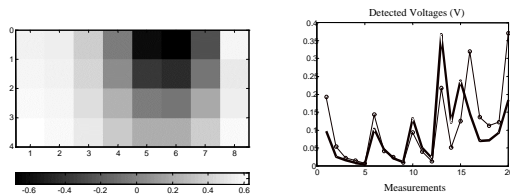
**Figure 13: Measured apparent resistivities. a) Normalised apparent resistivity. b) Apparent resistivity for the tube (thin line) and for the tube plus simulated water leak (thick line).**



**Figure 16: Measured apparent resistivities. a) Normalised apparent resistivity. b) Apparent resistivity for the tube (thin line) and the simulated leak (thick line).**

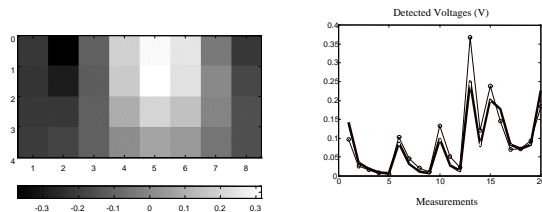
**4.2. Results using the dipole-dipole array**

Figure 14 shows the reconstructed images and measured voltages for the tube alone using the dipole-dipole array, including voltages measured by the end electrodes. Circles correspond to voltages measured on the reference area. The thick line corresponds to voltages measured along an imaginary surface line across the tube and perpendicular to its axis. All measured voltages are smaller than those measured using the modified Schlumberger array (figure 11b).



**Figure 14: a) Reconstructed image for the tube using the dipole-dipole array. b) Measured voltages for the reference area (circles) and on the area where there is the buried tube (thick line).**

Figure 15 shows the measured voltages and the reconstructed image for the simulated water leak. The image area close to the tube again changes in colour, pointing to a more conductive medium as result of the leak.



**Figure 15: a) Reconstructed image for the simulated leak using the dipole-dipole array. b) Measured voltages when there is a simulated leak (thick line).**

Figure 16 shows measured apparent resistivities for the tube and the simulated leak, and the normalised apparent resistivity. Here too, negative apparent resistivity values imply a leak that is more conductive than the tube.

Both electrode arrays yield similar results. Both locate the tube in its approximate position and the presence of a leak close to it. (Voltage measurements were taken immediately after pouring water, and therefore the leak did not have time to spread.)

The leak has been detected using as reference measurements those corresponding to the tube alone. Hence, the electrodes stayed in place, which guarantees similar measurement conditions.

Both the reconstructed images and the apparent resistivity curves indicate that the leak is more conductive than the tube. The availability of apparent resistivity curves helps in ensuring that the reconstructed images are not the result of some uncontrolled artefact.

**5. CONCLUSIONS**

Kotre [6] proposed a reconstruction algorithm to image impedance distributions based on the sensitivity theorem that does not need any regularisation parameter. We have applied this algorithm to detect underground leaking pipes using 16 and 8 electrodes, and the dipole-dipole and a modified Schlumberger array. Laboratory measurements for a simulated non-conductive leak show that leak detection is possible by using as reference voltages those measured for the non-leaking pipe. This is convenient because small changes in electrode position have a strong influence in the reconstructed images. Field measurements have allowed us to detect a simulated conductive leak from an insulating tube. The similitude between images reconstructed from each electrode array validates the method.

Increasing the number of electrodes and reducing their separation would improve image resolution. Bidimensional arrays could provide data to image horizontal layers.

## REFERENCES

- [1] R. H. Burger, "Exploration geophysics of the shallow subsurface", Englewood Cliffs (NJ): Prentice Hall, 1992.
- [2] K.A. Dines, R.J. Lytle, "Analysis of electrical conductivity imaging", *Geophysics*, 1981, 46, 7, pp. 1025-1036.
- [3] A.N. Tikhonov, A.V. Goncharsky, "Ill-posed problems in the natural sciences", Moscow: MIR, 1987.
- [4] E. Orellana, "Prospección Geoeléctrica en corriente continua", 2<sup>nd</sup> ed. Madrid: Paraninfo, 1982.
- [5] D.C. Barber, "Quantification in impedance imaging", *Clin. Phys. Physiol. Meas.*, 1990, 11 supl. A, pp. 45-56.
- [6] C.J. Kotre, "Studies of image reconstruction methods for electrical impedance tomography", PhD thesis. University of Newcastle-Upon-Tyne, UK, 1993.
- [7] M. Noel, B. Xu, "Archaeological investigation by electrical resistivity tomography: a preliminary study", *Geophys. J. Int.*, 1991, 107, pp. 95-102.
- [8] L.R. Lines, S. Treitel, "Tutorial. A review of least-squares inversion and its application to geophysical problems", *Geophysical Prospecting*, 1984, 32, pp. 159-186.
- [9] W. Menke, "Geophysical data analysis: discrete inverse theory", London: Academic Press, 1989.
- [10] D. Kahaner, C. Moler, S. Nosh, "Numerical Methods and Software". Englewood Cliffs (NJ): Prentice Hall, 1989.
- [11] P. Lascaux, R. Theodor, "Analyse numérique matricielle appliquée à l'art de l'ingénieur", Paris: Mason, 1986.
- [12] M.H. Loke, Torleif Dahlin, "A comparison of different least-squares formulations for the inversion of resistivity and IP Data", IV Meeting of the Environmental and Engineering Geophysical Society. Barcelona 14-17.september, 1998, pp. 825-828.
- [13] D.B. Geselowitz, "An application of electrocardiographic lead theory to impedance pletysmography", *IEEE Trans. Biomed. Eng.*, 1971, 18, pp. 38-41.
- [14] C.J. Kotre, "EIT image reconstruction using sensitivity weighted filtered backprojection". *Physiol. Meas.*, 1994, 15, pp. A125-A136.
- [15] C.J. Kotre, "Subsurface electrical impedance imaging using orthogonal linear electrode arrays" *IEE Proc, Meas. Technol.*, 1996, vol. 143,1, pp. 41-46.
- [16] C.J. Kotre, "Detection of sub-surface objects by electrical impedance tomography. Detection of abandoned land mines", *IEE Conference Publication*, 7-9 october 1996, pp. 67-71.
- [17] M. Gasulla, J. Jordana, R. Pallás-Areny, J.M. Torrents, "Subsurface resistivity measurements using square waveforms", *IEEE Instrumentation and Measurement Technology Conference*, May 19-21, 1997, Ottawa, Canada, pp. 1252-1256.
- [18] I. García, "Differential synchronous detector for soil electrical resistivity measurement", *Proyecto fi de carrera, ETSETB, UPC*, (In Spanish), 1998.
- [19] M. Gasulla, J. Jordana, R. Pallás-Areny, J.M. Torrents, "A fully differential synchronous demodulator." *Proceedings DCIS'96*, November 20-22. Sitges, Barcelona, 1996.
- [20] F. LL. Llorens, "Automated system for soil resitivity measurement", *Proyecto final de carrera, ETSETB, UPC*, (In Catalan), 1998.
- [21] J. Jordana, M. Gasulla, R. Pallás-Areny. "Depth and size determination of concentric cylindrical anomalies applied to leak detection in buried pipes", IV Meeting of the Environmental and Engineering Geophysical Society, September 14-17, Barcelona, 1998, pp. 553-556.
- [22] M. Gasulla, J. Jordana, R. Pallás-Areny, "Automated electrical impedance measuring systems to detect leaks from buried pipes", IV Meeting of the Environmental and Engineering Geophysical Society. Barcelona, September 14-17, 1998, pp. 809-812.
- [23] M. Gasulla, J. Jordana, R. Pallás-Areny, "Subsurface resistivity imaging using two single-step algorithms", IV Meeting of the Environmental and Engineering Geophysical Society, Barcelona, September 14-17, 1998, pp. 291-294.
- [24] J. Sánchez. "Imaging underground impedance distributions to detect leaking buried pipes and tanks", *Proyecto final de carrera, ETSETB, UPC*, (In Spanish), 1998.